Korean J. Chem. Eng., 35(11), 2283-2289 (2018)
DOI: 10.1007/s11814-018-0122-9

pISSN: 0256-1115
eISSN: 1975-7220

Template-free preparation of TiO_2 microspheres for the photocatalytic degradation of organic dyes

Mouza Al Ruqaishy*, Faisal Al Marzouqi*, Kezhen Qi, Shu-yuan Liu***, Sreejith Karthikeyan****, Younghun Kim*****, Salma Mohamed Zahran Al-Kindy*, Alex Tawanda Kuvarega******, and Rengaraj Selvaraj*,†**

*Department of Chemistry, College of Science, Sultan Qaboos University, Muscat, Sultanate of Oman
**Institute of Catalysis for Energy and Environment, College of Chemistry and Chemical Engineering, Shenyang Normal University, Shenyang, 110034, China
***Department of Pharmacology, Shenyang Medical College, Shenyang City, Liaoning Province 110034, China
****Department of Physics and Nanotechnology, SRM Research Institute, SRM University, Kattankulathur, Tamil Nadu - 603 203, India
*****Department of Chemical Engineering, Kwangwoon University, 20 Kwangwoon-ro, Nowon-gu, Seoul 01897, Korea
******Nanotechnology and Water Sustainability Research Unit, College of Science, Engineering and Technology, University of South Africa, Florida Science Campus, Johannesburg, South Africa
(*Received 2 April 2018 • accepted 18 July 2018*)

Abstract−TiO_2 microspheres were successfully synthesised by simple solution phase method by using various amount of titanium butoxide as precursor. The prepared TiO_2 were characterized by X-ray diffraction (XRD), UV-vis diffuse reflectance absorption spectra (UV-DRS), X-ray photoelectron spectroscopy (XPS) and scanning electron microscopy (SEM). XRD analysis revealed that the as-synthesized TiO_2 microsphere poses an anatase phase. The photocatalytic degradation experiments were carried out with three different dyes, such as methylene blue, brilliant black, reactive red-120 for four hours under UV light irradiation. The results show that TiO_2 morphology had great influence on photocatalytic degradation of organic dyes. The experimental results of dye mineralization indicated the concentration was reduced by a high portion of up to 99% within 4 hours. On the basis of various characterization of the photocatalysts, the reactions involved to explain the photocatalytic activity enhancement due to the concentration of titanium butoxide and morphology include a better separation of photogenerated charge carriers and improved oxygen reduction inducing a higher extent of degradation of aromatics.

Keywords: TiO_2, Template-free, Hydrothermal, Photocatalytic Activity, Organic Dye

INTRODUCTION

The presence of organic contaminants in water is currently an environmental concern globally. Large amounts of dyes are produced annually from the textile, cosmetic, paper, leather, pharmaceutical and food processing industries [1,2]. In the textile manufacturing process, dyes are generated during the scouring, bleaching, dyeing, rinsing, washing and finishing processes to result in wastewater effluent of different chemical, color and organic content [3]. Some of these dyes are toxic and mutagenic and also reduce light penetration in aquatic systems for photosynthetic processes [4].

Advanced dye wastewater treatment technologies, capable of completely degrading the dyes to harmless by-products are the focus of current research efforts in this field. Conventional methods, such as adsorption, coagulation, flocculation, biological and membrane technologies or their integration, have resulted in appreciable success in removal of reactive dyes from textile wastewaters [5]. Adsorption and membrane processes are largely non-destructive and thus dye molecules are transferred from the liquid to the solid phase [6]. Biological processes are compromised because of the high stability, low biodegradability, high toxicity of synthetic dyes and the presence of large quantities of aromatics in the dye effluent [7].

In the last few decades, new technologies potentially capable of completely eliminating organic compounds in water have emerged. Advanced oxidation processes (AOPs) have been reported to non-selectively oxidise a broad range of organic pollutants [8]. Among the AOPs, heterogeneous photocatalysis has proved popular due to the photostability, chemical and biological inertness, ready availability and low cost of semiconductors such as TiO_2 [9,10]. Nano sized TiO_2 with desirable properties such as high crystallinity, small crystallite size, high specific surface area and porous structures has been successfully synthesized and applied in degradation of various organic compounds in water [11].

Recently, azo dyes Rhodamine B and Methyl orange were degraded using TiO_2 under simulated solar radiation in a binary system [12]. In another study, F, N and S tri-doped TiO_2 thin films immobilized on the glass spheres were evaluated for the degradation of textile industry pollutants, and 86-100% removal were achieved within 6 hrs of visible irradiation [13]. High surface area meso-

†To whom correspondence should be addressed.
E-mail: rengaraj@squ.edu.om

porous TiO_2 (40.03 m^2/g) was synthesized via a sol-gel route using butyl titanate as a precursor. The synthesized TiO_2 with a pore diameter of about 13.04 nm exhibited excellent photocatalytic activity towards the degradation of organic pollutants in tannery wastewater under UV-light and natural sunlight irradiation [14]. Khanna and Shetty [15], recently synthesized Ag core-TiO_2 shell nanoparticles of approximately 30 nm via a one pot route. The photocatalyst was evaluated for its effectiveness in the degradation of Reactive Blue 220 under UV and visible light irradiation and a higher degradation rate was observed under visible light irradiation.

Although, application of nano TiO_2 in environmental remediation has achieved some successes, there are still challenges with stability of the nanoparticles at the nanometer scale. Also, the particles tend to agglomerate at that scale. Another challenge is removal of the nanoparticles from the slurry solutions after the photocatalytic reaction [16]. To overcome these challenges, high surface area supports have been used to disperse the photocatalyst in the reaction medium. An interesting innovation is the synthesis of porous TiO_2 microspheres which can be fabricated into monodisperse porous beads or polymeric templates with controlled morphological properties such as pore size, outer shape and size [17]. Moreover, recent studies have shown promising results of TiO_2 microspheres samples with more enhanced performance compared to a standard conventional sample such as P25 [18,19].

The aim of this study was to develop a template-free solution phase synthesis of TiO_2 microspheres for the decolorization/degradation of azo dyes. Recently, methylene blue, brilliant black, methyl orange and reactive red 120 have been accepted as model dyes for the investigation of their degradation and adsorption processes. However, their degradation mechanisms are still unknown. In this work, TiO_2 microspheres were prepared by a template-free solution phase method. Photocatalytic degradation experiments were then carried out using three different dyes, methylene blue, brilliant black and reactive red-120, for four hours under UV light irradiation. The results showed that TiO_2 morphology had great influence on the photocatalytic degradation of the organic dyes.

EXPERIMENTAL

Analytical grade titanium butoxide ([$Ti(BuO)_4$], 99%), ethanol (EtOH, 99%), were purchased from Sigma-Aldrich and used as received without additional purification. The dye sample methylene blue (MB), brilliant black (BB) and reactive red 120 (RR 120) were obtained from the Sigma-Aldrich and used without further purification. Deionized, double distilled water was used for the preparation of all solutions.

In a typical procedure for the synthesis of TiO_2 microsphere, various amount of 1, 2, 3 and 5 mL of titanium butoxide were dissolved in 75 mL of EtOH and continuously stirred for overnight by passing the air with the help of aerator at room temperature in a 250 mL conical flask. In template-free method during hydrolysis, the liquid was kept under continuous stirring for overnight. After that, the white powder obtained was dried at 80 °C in an oven for 12 h and then calcined at 450 °C for 3 h for further characterization.

The crystalline properties of TiO_2 nanocrystals were studied by X-ray diffraction (XRD) using a bench X-ray diffractometer (MiniFlex 600). X-ray diffractometer was equipped with graphite monochromatized CuK_α radiation (λ=1.54056 Å). The absorption spectra of the as-prepared samples were recorded using UV-Vis diffuse reflectance spectroscopy (DRS, Jasco V670) in the wavelength range of 200-1,000 nm, with $BaSO_4$ as a reference. The morphology of the microspheres was characterized by field-emission scanning electron microscopy (Jeol, JSM 7600F). The chemical states and relative compositions of the samples were studied by X-ray photoelectron spectroscopy (XPS, Omicron Nanotechnology) with a monochromatized AlK_α irradiation (1.4867 eV) and a pass energy of 20 eV. All XPS spectra were obtained with an energy step of 0.1 eV and a dwell time of 50 ms. A software package (Casa Software Ltd) has been used to analyze the XPS data.

All photoreaction experiments were carried out in a photocatalytic reactor system, which consists of a cylindrical borosilicate glass reactor vessel with an effective volume of 250 mL, a cooling water jacket, and a UV-B lamp (8 W medium-pressure mercury lamp, Institute of Electric Light Source) positioned axially at the center as a visible light. The reaction temperature was kept at 25 °C by circulating the cooling water. A special glass frit as an air diffuser was fixed at the reactor to uniformly disperse air into the solution. Photocatalytic activity of the prepared samples was examined by the degradation of Methylene Blue, Brilliant Black and Reactive Red 120 under UV-B light irradiation. For each run the reaction suspension was freshly prepared by adding 0.250 g of catalyst into 250 mL of aqueous Methylene Blue and Brilliant Black solutions with an initial concentration of 5 mg L^{-1} and adding 0.050 g of catalyst into 250 ml of aqueous Reactive Red 120 solution with an initial concentration of 5 mg/L. After the degradation, all samples were filtered using syringe and syringe filter 0.45 μm to remove any precipitated particles. The filtrate was analyzed by an UV-vis absorption spectra instrument. The absorption spectra were recorded using an UV-vis spectrophotometer (UC-2450-SHIMADZU). The maximum characteristic absorption wavelengths of MB, BB and RR120 were positioned at 664, 570 and 512 nm, respectively.

RESULTS AND DISCUSSION

The as-prepared TiO_2 microsphere samples were analyzed by using XRD measurements which are deposited with various amount of titanium butoxide with 1, 2, 3 and 5 mL in content shown in Fig. 1. It is clear from the analysis that these microspheres prefer anatase phase with the presence of (101), (103), (004), (112), (200), (105), (211), (213), (116), (220) and (215). These peaks match exactly with the reported JCPDS No. 21-1272 corresponding to the anatase phase of TiO_2. The y axis scale was fixed same for the entire sample. TiO_2 especially in the anatase form, is very well known for its photo-catalyst activity with under ultraviolet (UV) light [20]. The (101) peak intensity increased up to 3 mL and it was reduced for 5 mL samples. The crystallite size of the synthesized TiO_2 samples was calculated from the full width at half maximum (FWHM) of the diffraction peaks using the Debye-Scherrer formula:

$$D = \frac{\alpha\lambda}{\beta\cos\theta}$$

where D is the mean crystallite size, α is a geometric factor (here,

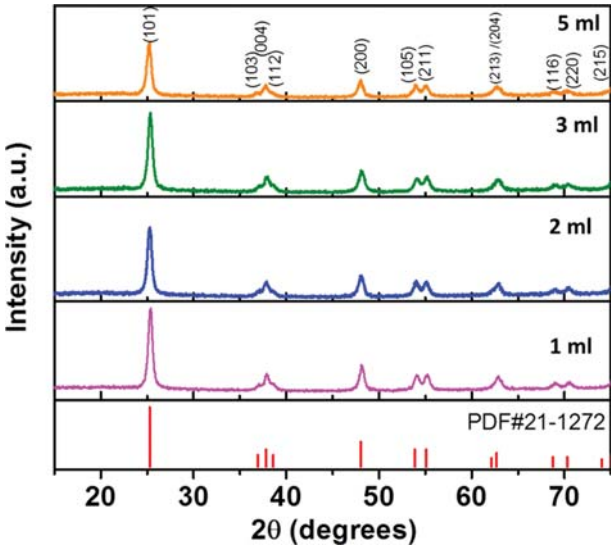

Fig. 1. X-ray diffraction pattern of TiO_2 microspheres prepared with different titanium butoxide.

α=1), λ is the wavelength of X-rays used for the diffraction measurements (here, λ=1.54065 Å), β is the FWHM of the diffraction peaks, which can be measured from the XRD peaks, and θ is the diffraction angle. The crystallite size of synthesized TiO_2 was 14, 14, 15, 15 nm for 1, 2, 3 and 5 ml titanium butoxide samples, respectively.

Bandgap energy of the samples was determined using diffuse reflectance measurements by UV-vis DRS spectrophotometer. The band gap value was determined by Kubelka-Munk (K-M or F(R)) method [21,22]. In this method, F(R) is proportional to the absorption coefficient α according to the following relationship:

$$F(R)=\frac{(1-R)^2}{2R}$$

where R is the reflectance. This relation is applied to highly light scattering materials and absorbing particles in a matrix. The dependence of absorption coefficient (α) on the photon energy equation is given as follows:

$$\alpha h\nu = A(h\nu - E_g)^m$$

where h is Planck's constant and v is frequency, E_g the band gap energy, and A is the constant having separate values for different transitions. The values of m for allowed direct, allowed indirect, forbidden direct, and forbidden indirect transition are 1/2, 2, 3/2, and 3, respectively. So, for our analysis we used m=2 for indirect band gap material. Since α is proportional to F(R) we plotted $(F(R)\cdot h\nu)^{1/2}$ v/s hv for finding the indirect band gap from the UV DRS data (Fig. 2(a)). The reported value for anatase phase TiO_2 is around 3.2 eV [23]. The prepared samples showed band gap values close to 2.9 eV. The band gaps increased from 2.83 eV to 2.93 eV up to 3 ml of titanium butoxide dosage; after that it decreased to 2.88 eV for the 5 ml sample. However, the indirect transition fitting plot for the TiO_2 samples yielded bandgap values less than the range accepted for TiO_2 anatase, which is 3 to 3.2 eV. This kind of result has been observed and reported previously [24]. The decline in the band gap value can be attributed mainly to smaller crystal-

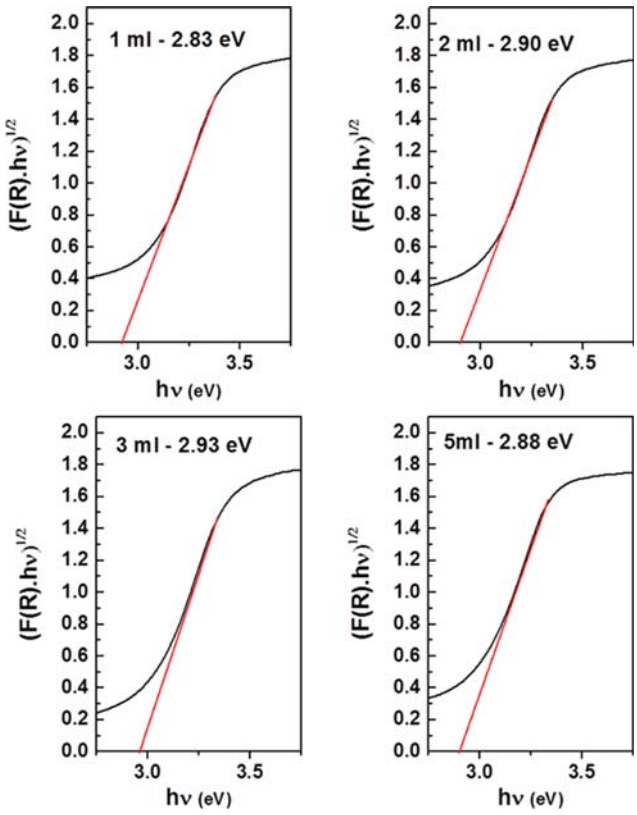

Fig. 2. Indirect transition Band-gap energy calculation of as-made TiO_2 microspheres.

lite size exhibited by the prepared samples. Due to quantum size effect, it is known that the recombination pathway of excited electrons in anatase phase cannot go via the same pathway used for indirect transition [25]. Thus, the data were fitted again to the direct bandgap transition (Fig. 3). The result showed that the direct transition plots are more appropriate with a value of 3.21, 3.19, 3.18 and 3.17 eV for 1, 2, 3 and 5 ml titanium butoxide samples.

The general survey and high resolution scans of XPS results are shown in Fig. 4. The XPS survey scan show the presence of Ti and O. There is also a carbon peak present in the scan which is from the background data from the carbon tape. This analysis confirms only the presence of titanium and oxygen. Our XPS results did not show any impurity for samples collected from difference sources at a detection limit of 0.05 at%. The Ti $2p_{1/2}$ and Ti $2p_{3/2}$ spin-orbital splitting photoelectrons for both samples are located at binding energies of 464.8 and 459.0 eV, respectively. The peak separation value of 5.8 eV was observed and it is very close to the reported values [26,27]. O 1s peak was located 530.2 eV, which is also very close to the reported value [28].

The SEM analysis shows the microsphere nature of the TiO_2 particles (Fig. 5). It is clear from the image that the particle size increased with increase in the precursor concentration. The particle size distribution was analyzed using Image J. 25 locations from each SEM image were selected and particle size distribution plotted for each condition. The statistical analysis showed that the average diameters of the spheres were 1.14±0.02 μm and 2.3±0.1 μm for the 2 ml and 3 ml precursor volumes, respectively.

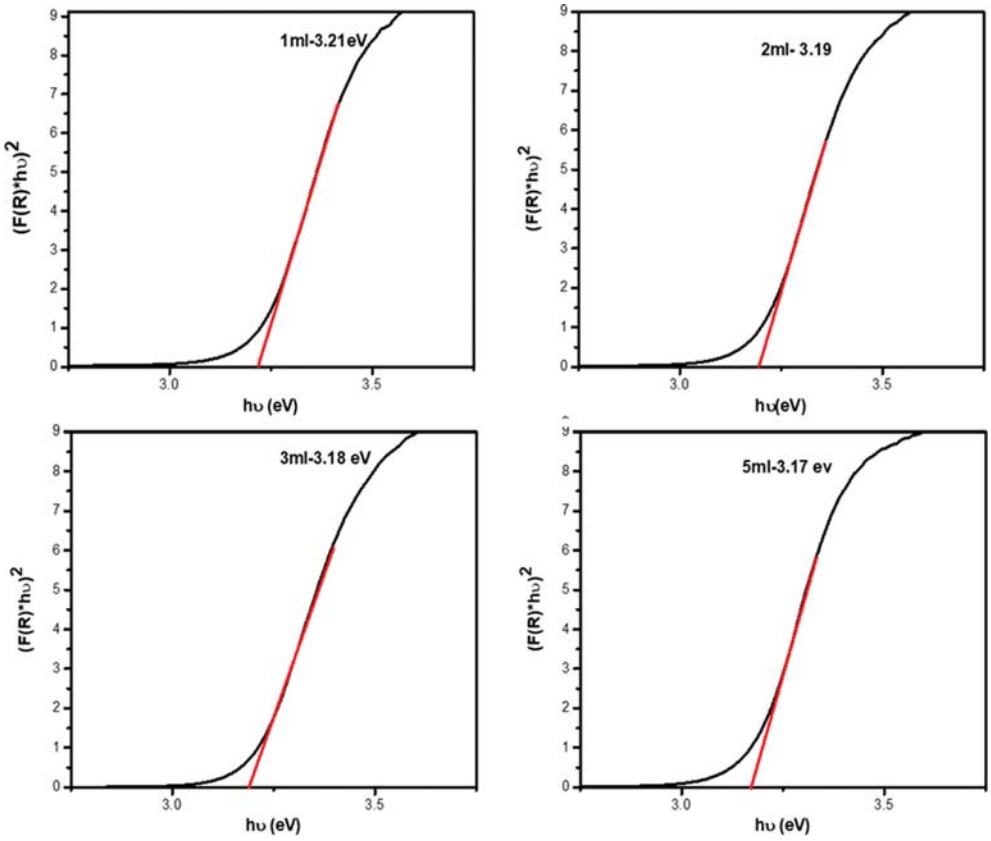

Fig. 3. Direct transition Band-gap energy calculation of as-made TiO_2 microspheres.

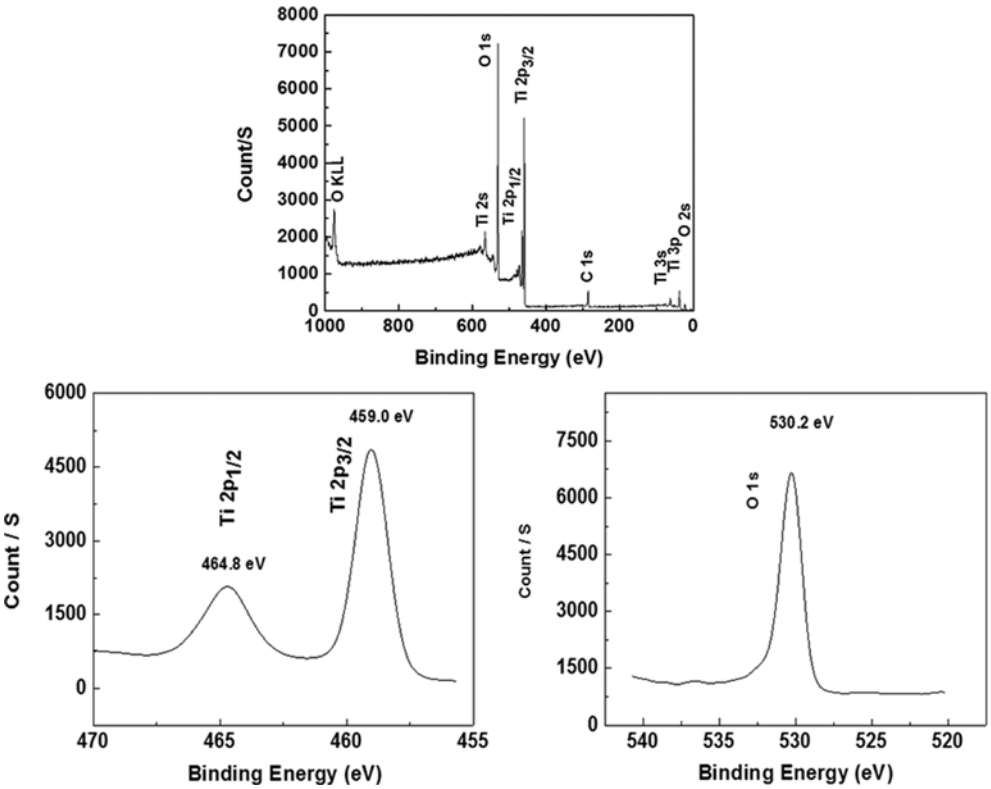

Fig. 4. XPS survey spectrum and high resolution spectra of TiO_2 microspheres (Ti 2p, O 1s).

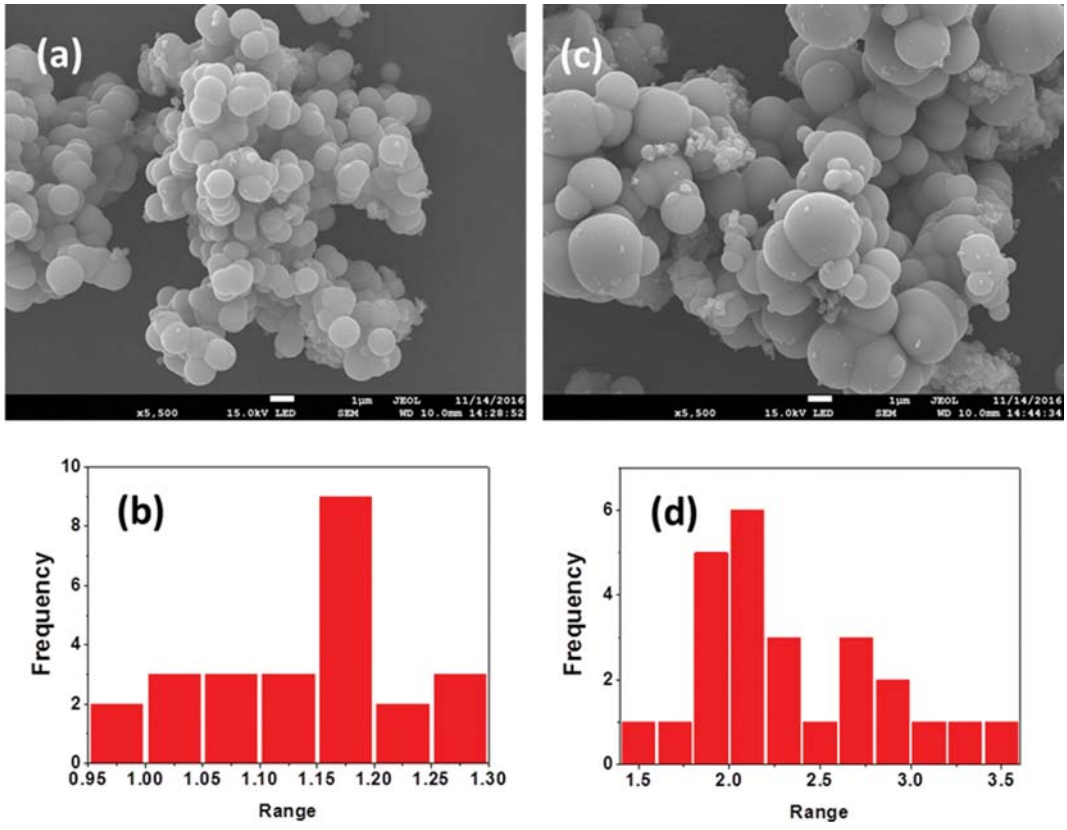

Fig. 5. SEM morphological analysis of TiO_2 microspheres, which was prepared with (a) 2 and (c) 3 mL titanium butoxide, and ((b) and (d)) their particle size distribution in μm.

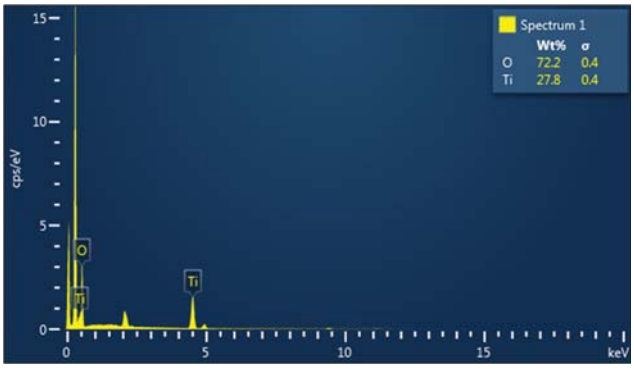

Fig. 6. EDS spectra of the TiO_2 microsphere.

The elemental analysis of the TiO_2 microsphere samples was performed by EDS analysis; the typical spectra of the TiO_2 microspheres are shown in Fig. 6. The EDS spectra recorded for all samples are identical, indicating that all samples have the same composition. The analysis confirmed that there are no elements other than Ti and O present in the sample [29,30].

Methylene blue, Brilliant black and Reactive red 120 are kind of organic dyes, and often used as model pollutant to study the photocatalytic activity or performance of nanomaterials. The maximal absorptive energy of Methylene blue, Brilliant black and Reactive red 120 is at 664, 570, and 512 nm, respectively. In this study, Methylene blue, Brilliant black and Reactive Red 120 were chosen as an object to investigate the photocatalytic degradation properties of them using prepared TiO_2 microspheres with the help of UV-vis adsorption spectra. From the figures, it is found that the absorptive intensity of Methylene blue (Fig. 7), Brilliant black (Fig. 8) and Reactive red 120 (Fig. 9) at 664, 570, and 512, respectively, gradually decreased with prolonging the irradiation time when the mixed solution of dyes and TiO_2 microspheres were exposed to UV-B light irradiation at room temperature.

These results indicated that these dyes underwent obvious degradation behavior under the catalysis of TiO_2 microspheres. If the degradation ratio is defined as the ratio between the decreased peak intensity and that of initial dye solution, the degradation ratio was about 99% when the dye solution was irradiated for 60 min with Methylene Blue, 40 min with Reactive Red and 10 min only with Brilliant Black. These imply that the as-synthesized TiO_2 microspheres have good photocatalytic activity for dyes and are likely to be efficient photocatalysts in the applied field.

CONCLUSIONS

An easy method was used to fabricate TiO_2 microspheres in a single step process without using any template. This study showed that the catalyst's resulting morphology, structure and photocatalytic properties are dependent on the concentration of precursor. The as-synthesized TiO_2 microspheres possess anatase phase with

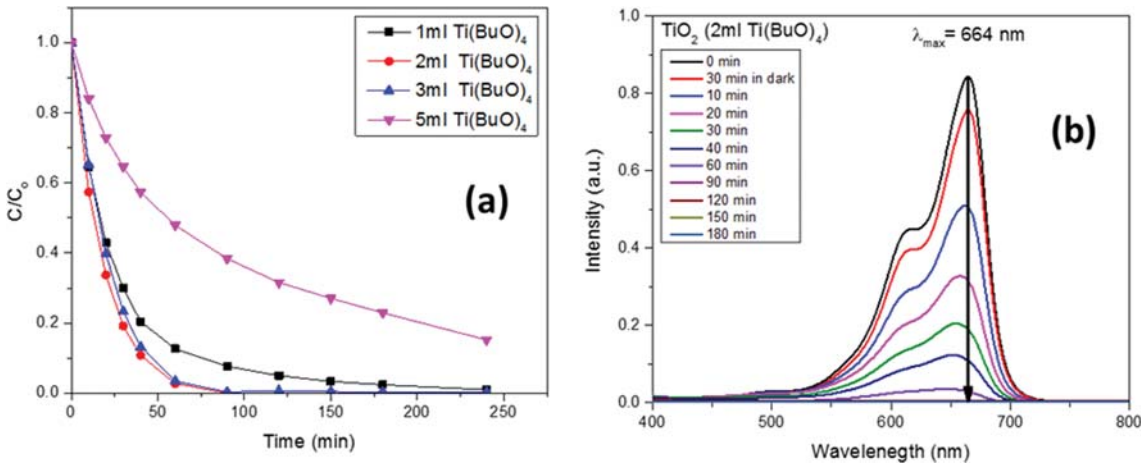

Fig. 7. Photocatalytic degradation of methylene blue by different TiO_2 microspheres. (a) Variation of normalized concentration of MB (C_0= 5 mg/L) with irradiation time under UV-light condition. (b) Time dependent UV-vis absorption spectrum of MB in the presence of TiO_2 - 2 mL (catalyst dosage - 250 mg/250 mL; concentration of MB=5 mg/L; pH=4.4; light source=UV-B).

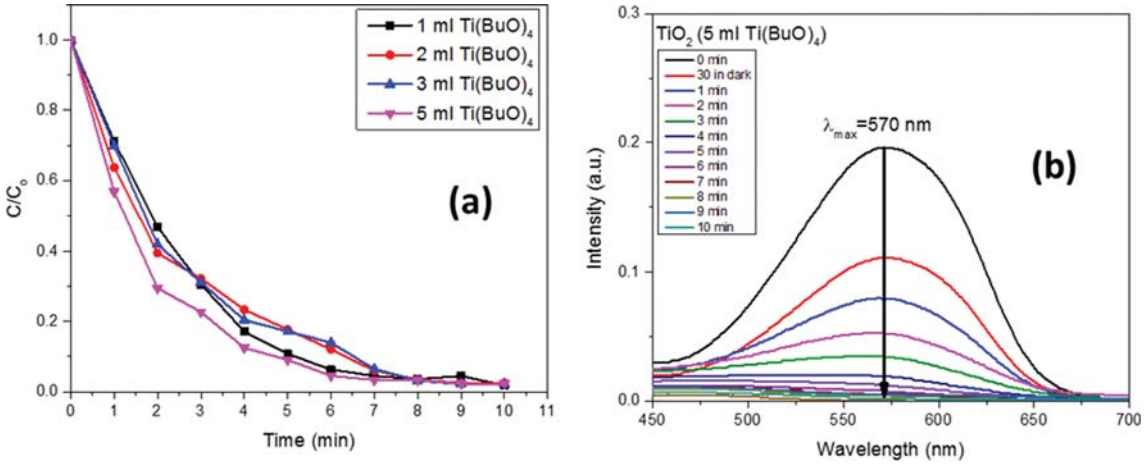

Fig. 8. Photocatalytic degradation of brilliant black by different TiO_2 microspheres. (a) Variation of normalized concentration of BB (C_0= 5 mg/L) with irradiation time under UV-light condition. (b) Time dependent UV-vis absorption spectrum of BB in the presence of TiO_2 - 1 mL (catalyst dosage - 250 mg/250 mL; concentration of BB=5 mg/L; pH=7.5; light source=UV-B).

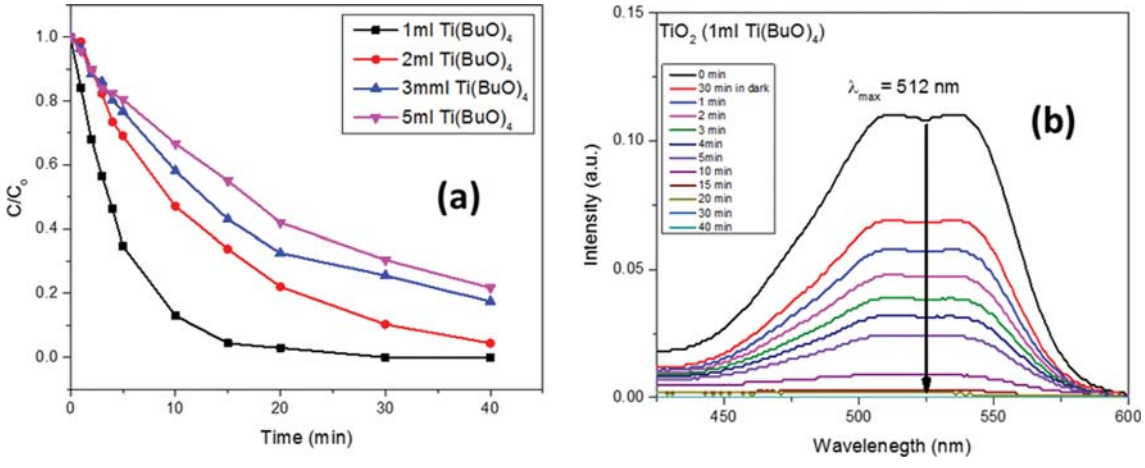

Fig. 9. Photocatalytic degradation of reactive red 120 by different TiO_2 microspheres. (a) Variation of normalized concentration of RR-120 (C_0=5 mg/L) with irradiation time under UV-light condition. (b) Time dependent UV-vis absorption spectrum of RR120 in the presence of TiO_2 - 5 mL (catalyst dosage - 50 mg/250 mL; concentration of RR120=5 mg/L; pH=7.5; light source=UV-B).

the size ranging from 1 to 3 μm. The EDX and XPS analysis also confirmed that there are no elements other than Ti and O, indicating the purity of the prepared samples. The photocatalytic degradation experiments were carried out with three different dyes, including methylene blue, brilliant black and reactive red-120 under UV light irradiation. The experimental results of dye mineralization indicated the concentration was reduced by a high portion of up to 95% within 4 hours. On the basis of various characterization of the photocatalysts, the reactions involved to explain the photocatalytic activity enhancement due to the concentration of titanium butoxide and morphology include a better separation of photogenerated charge carriers and improved oxygen reduction inducing a higher extent of degradation of aromatics.

ACKNOWLEDGEMENTS

This study was supported by SQU-UAEU joint research project (CL/SQU-UAEU/16/04).

REFERENCES

1. N. M. Mahmoodi, J. Abdi, M. Oveisi, M. A. Asli and M. Vossoughi, *Mater. Res. Bull.*, **100**, 357 (2018).
2. A. R. Khataee and M. B. Kasiri, *J. Mol. Cat. A*, **328**, 8 (2010).
3. M. C. V. M. Starling, L. A. S. Castro, R. B. P. Marcelino, M. M. D. Leão and C. C. Amorim, *Environ. Sci. Pollut. Res.*, **24**, 6222 (2017).
4. F. S. Domingues, T. K. F. S. Freitas, C. A. de Almeida, R. P. de Souza, E. Ambrosio, S. M. Palácio and J. C. Garcia, *Environ. Technol.*, 1 (2017), DOI:10.1080/09593330.2017.1418913.
5. N. Jaafarzadeh, A. Takdastan, S. Jorfi, F. Ghanbari, M. Ahmadi and G. Barzegar, *J. Mol. Liq.*, **256**, 162 (2018).
6. R. P. Souza, T. K. Freitas, F. S. Domingues, O. Pezoti, E. Ambrosio, A. M. Ferrari-Lima and J. C. Garcia, *J. Photochem. Photobio.* A, **329**, 9 (2016).
7. A. Asghar, A. A. A. Raman and W. M. A. W. Daud, *J. Clean. Prod.*, **87**, 826 (2015).
8. A. Touati, T. Hammedi, W. Najjar, Z. Ksibi and S. Sayadi, *J. Ind. Eng. Chem.*, **35**, 36 (2016).
9. H. U. Farouk, A. A. A. Raman and W. M. A. W. Daud, *J. Ind. Eng. Chem.*, **33**, 11 (2016).
10. M. E. Borges, M. Sierra, E. Cuevas, R. D. García and P. Esparza, *Sol. Energy*, **135**, 527 (2016).
11. K. M. Reza, A. S. W. Kurny and F. Gulshan, *Appl. Water Sci.*, **7**, 1569 (2017).
12. D. Ariyanti, M. Maillot and W. Gao, *J. Environ. Chem. Eng.*, **6**, 539 (2018).
13. M. Behpour, R. Foulady-Dehaghi and N. Mir, *Sol. Energy*, **158**, 636 (2017).
14. W. Zhao, X. He, Y. Peng, H. Zhang, D. Sun and X. Wang, *Water Sci. Technol.*, **75**, 1494 (2017).
15. A. Khanna and V. K. Shetty, *Sol. Energy*, **99**, 67 (2014).
16. S. Park, W. Kim and Y. Kim, *Korean J. Chem. Eng.*, **34**, 1500 (2017).
17. K. Ö. Hamaloğlu, E. Sağ, A. Bilir and A. Tuncel, *Mater. Chem. Phys.*, **207**, 359 (2018).
18. C. Wang, H. Liu, Y. Liu, G. He and C. Jiang, *Appl. Surf. Sci.*, **319**, 2 (2014).
19. C. J. Lin, W.-T. Yang, C.-Y. Chou and S. Y. H. Liou, *Chemosphere*, **152**, 490 (2016).
20. X. Chen and S. S. Mao, *Chem. Rev.*, **107**, 2891 (2007).
21. P. Kubelka and F. Munk, *Tech. Phys.*, **12**, 593 (1931).
22. P. Kubelka, *J. Opt. Soc. Am.*, **38**, 448 (1948).
23. H. Tang, K. Prasad, R. Sanjines, P. Schmid and F. Levy, *J. Appl. Phys.*, **75**, 2042 (1994).
24. K. M. Reddy, S. V. Manorama and A. R. Reddy, *Mater. Chem. Phys.*, **78**, 239 (2003).
25. J. Zhang, P. Zhou, J. Liu and J. Yu, *Phys. Chem. Chem. Phys.*, **16**, 20382 (2014).
26. B. Erdem, R. A. Hunsicker, G. W. Simmons, E. D. Sudol, V. L. Dimonie and M. S. El-Aasser, *Langmuir*, **17**, 2664 (2001).
27. A. R. Burke, C. R. Brown, W. C. Bowling, J. E. Glaub, D. Kapsch, C. M. Love, R. B. Whitaker and W. E. Moddeman, *J. Surf. Interface Anal.*, **11**, 353 (1988).
28. H.-A. Park, S. Liu, Y. Oh, P. A. Salvador, G. S. Rohrer and M. F. Islam, *ACS Nano.*, **11**, 2150 (2017).
29. F. Wang, J. H. Ho, Y. Jiang and R. Amal, *ACS Appl. Mater. Interf.*, **7**, 23941 (2015).
30. S. H. Sharif and A. R. Aldo, *Ind. Eng. Chem. Res.*, **47**, 6598 (2008).